EVOLUTIONARY ECOLOGY

Adaptation and gene flow are insufficient to rescue a montane plant under climate change

Jill T. Anderson[1]†*, Megan L. DeMarche[2]†*, Derek A. Denney[2], Ian Breckheimer[3,4], James Santangelo[5], Susana M. Wadgymar[6]

Climate change increasingly drives local population dynamics, shifts geographic distributions, and threatens persistence. Gene flow and rapid adaptation could rescue declining populations yet are seldom integrated into forecasts. We modeled eco-evolutionary dynamics under preindustrial, contemporary, and projected climates using up to 9 years of fitness data from 102,272 transplants (115 source populations) of *Boechera stricta* in five common gardens. Climate change endangers locally adapted populations and reduces genotypic variation in long-term population growth rate, suggesting limited adaptive potential. Upslope migration could stabilize high-elevation populations and preserve low-elevation ecotypes, but unassisted gene flow modeled with genomic data is too spatially restricted. Species distribution models failed to capture current dynamics and likely overestimate persistence under intermediate emissions scenarios, highlighting the importance of modeling evolutionary processes.

Climate change is rapidly shifting the geographic distributions of species (*1*, *2*), owing to changes in local population dynamics, which govern persistence, extirpation, and colonization (*3*). Determining how specific climatic factors causally affect population growth rates across a species' range could enable robust predictions of response to new climates (*3*–*5*). An even bigger, and as yet unmet, challenge, is to incorporate standing genetic variation, rapid adaptation, and gene flow into population models to forecast eco-evolutionary dynamics (*4*, *6*–*9*).

Evolutionary processes have the potential to substantially alter population persistence and distribution under climate change. Widely distributed species with broad climatic tolerances could have a greater potential to survive contemporary climate change than narrowly distributed specialists or species from regions with historically stable climates (*10*–*12*). However, many widespread species consist of mosaics of populations adapted to local conditions (*13*, *14*), and the climatic niche of individuals from a single population may represent only a small proportion of the tolerance of the species. Climate change is expected to increase extinction risks for populations at the warmer range edges of many species (*1*, *2*). However, for locally adapted species, selection imposed by climate change [e.g., (*15*, *16*)] could depress the fitness of local ecotypes (*17*–*21*) throughout the range ("local maladaptation"). Nevertheless, adaptive evolution to new climates could rescue declining populations and enable long-term persistence (*22*) given sufficient within-population genetic variation in climate tolerances ("evolutionary rescue") (*23*, *24*). Similarly, gene flow could enhance population persistence under climate change (*25*) by introducing alleles from populations adapted to new or future conditions ("genetic rescue"). Quantitative genetic field experiments that manipulate climatic factors hold great promise for evaluating the actual roles of eco-evolutionary processes in mitigating extinction risks.

We tested the contributions of local adaptation, migration of pre-adapted ecotypes, and in situ evolutionary rescue to predicted long-term population persistence under climate change in the ecological model species Drummond's rockcress (*Boechera stricta,* Brassicaceae), which is a short-lived perennial species common in montane meadows of North America (*26*) (Fig. 1, A to C, and figs. S1 and S2). High-elevation plants may be particularly susceptible to climate change [e.g., (*27*)] because mountainous ecosystems are subject to high rates of warming (*28*). We identified causal climatic factors that influence performance and characterized the spatial scale of local adaptation by manipulating snowpack and temperature in five common gardens across an elevational gradient around the Rocky Mountain Biological Laboratory (Gothic, Colorado, USA) in experiments using seeds and juvenile plants from inbred maternal lines (hereafter: genotypes). In the "Provenance Trial" experiments, we sampled genotypes that spanned a broad elevational gradient to examine local adaptation under four climate scenarios and quantify the degree of migration that would be necessary to keep pace with climate change. In the "Reciprocal Transplant" experiment, we transplanted genotypes local to each garden to characterize the climate niche and test the potential for in situ evolutionary rescue (*29*). We then leveraged population- and genotype-specific climate responses to develop integral projection models (IPMs) (*30*) capable of evaluating the contributions of evolutionary processes to population growth and persistence. Climatic tolerances are often assessed by comparing occurrence records to macroclimate layers or through short-term laboratory experiments focused on single climatic factors and metrics of performance (e.g., temperature and individual growth) (*31*). Our approach generates more robust assessments by integrating across life history and exposing transplants to complex suites of environments in ecologically realistic field conditions (fig. S3) to uncover the climate conditions in which population growth rate (λ) is positive (the "demographic niche"). Our design overcomes the constraints of space-for-time approaches, in which climatic conditions covary with other environmental factors, such as edaphic characteristics, and captures climates spanning preindustrial to forecasted conditions (Fig. 1 and figs. S1 to S4).

Provenance trial experiment reveals local maladaptation under climate change

To evaluate adaptational lag under climate change, we developed climate-driven stochastic IPMs (*30*), which examined how long-term population growth rates (λ_s) depend on climate as a function of source population elevation. Population growth rate (λ) is the appropriate measure of long-term fitness in constant environments when populations may be growing or declining, and λ_s is the appropriate fitness measure in variable environments (*32*). We transplanted multiple cohorts of 3-month old juveniles (N = 9840 individuals of 199 genotypes from 64 populations, 2013 and 2014) and seeds (N = 64,804 seeds of 285 genotypes from 99 populations, 2014, 2016, and 2018) collected across the elevational range (2499 to 3690 m) into five gardens (table S1). We exposed these individuals of known origin to ambient snowpack and early snow removal to simulate climate change. In two seed cohorts (2016 and 2018), we also examined germination success and seedling survival under snow addition, which reflects recent historical climates (*20*). Additionally, in 2018 and 2020, we factorially manipulated both snow dynamics (ambient versus early snowmelt) and growing season temperature (ambient versus elevated, using open-top chambers, table S2) to capture vital rates under a greater range of climates (N = 8880 juveniles of 96 genotypes from 57 populations, transplanted into four gardens in 2018 and five in 2020). However, snow removals and open-top chambers were not applied at the lowest garden for the 2020 cohort owing to poor performance of transplants in that site in recent years. In all experiments, we left the local vegetation intact and did not modify any other aspects of the environment; thus, transplants experienced the full suite of interacting abiotic and biotic

[1]Department of Genetics and Odum School of Ecology, University of Georgia, Athens, GA, USA. [2]Department of Plant Biology, University of Georgia, Athens, GA, USA. [3]Rocky Mountain Biological Laboratory, Gothic, CO, USA. [4]Western Colorado University, Gunnison, CO, USA. [5]Department of Integrative Biology, University of California, Berkeley, CA, USA. [6]Biology Department, Davidson College, Davidson, NC, USA. ***Corresponding author. Email: jta24@uga.edu (J.T.A.); megan.demarche@uga.edu (M.L.D.)** †These authors contributed equally to this work.

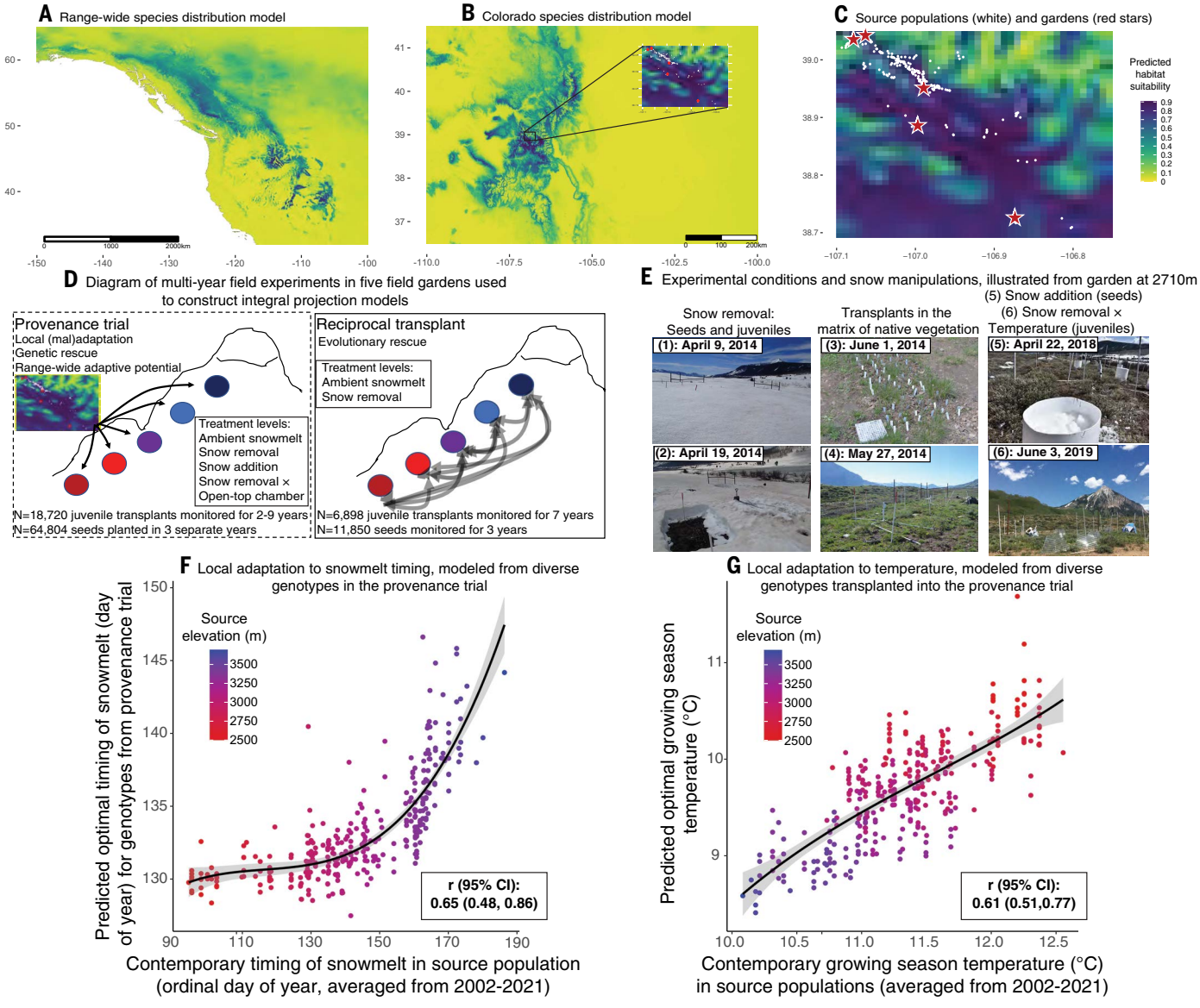

Fig. 1. Distribution and climatic adaptation of *Boechera stricta*. (**A**) Range-wide species distribution model showing regions of high (blue) versus low (yellow) habitat suitability based on correlations of occurrences and recent historical climatic data (1970–2000). Longitude is shown on the *x* axis and latitude on the *y* axis. (**B**) Species distribution model focused on Colorado, with an inset panel showing the locations of all source populations (white circles) and the five common gardens (red stars) used in field experiments. (**C**) Enlarged species distribution map of the source populations and gardens. (**D**) The provenance experiment exposed full siblings from inbred families originating from populations across a broad climatic gradient to variable climates in five experimental gardens. The reciprocal transplant included more genotypes from each garden, transplanted into all gardens. (**E**) Experimental conditions illustrated using images from a low-elevation garden. Photo 1: Immediately before snow removal. Credit: B. Chowdhury. Photo 2: Snow removal blocks were melted out while snow was intact in the control blocks. Credit: B. Chowdhury. Photo 3: Experimental individuals marked with unique identifiers and transplanted into the matrix of natural vegetation. Photo 4: Experimental blocks embedded in natural community, with PVC pipes delineating blocks and data loggers capturing soil moisture and temperature. Photo 5: Snow addition block visible in snow-free garden. Credit: Jillian Gall. Photograph 6: Data collection after establishment of open top chambers. Photos 3, 4, and 6: Credit: J. T. Anderson. (**F**) The optimal timing of snowmelt and (**G**) the optimal growing season temperature for each genotype in the provenance experiment versus the average climatic conditions modeled for each source population from 2002 to 2021, revealing local adaptation to climate (the data are from the Provenance Trial). Data points are colored by source elevation. Correlation coefficients (r) and 95% bias-corrected confidence intervals (CI) are given within each panel.

agents of selection in each garden (Fig. 1, D and E). We examined the entire *B. stricta* life cycle by monitoring seed germination and seedling recruitment of transplanted seeds for 1 year, along with survival, growth, and fecundity of transplanted rosettes from planting through the autumn of 2022.

To construct IPMs, we first analyzed how eight vital rates varied as a function of source elevation and fine-grained spatiotemporal variation in two climatic predictors reflecting energy budgets (average daily growing season temperature) and water availability and growing season timing (snowmelt timing), respectively (table S3 and figs. S5 to S9). These climatic drivers are key determinants of plant fitness at high elevations and latitudes (*33*) and are shifting rapidly with climate change globally (*34*–*36*) and in our study region (fig. S4). We incorporated population- and genotype-specific climate tolerances for each vital rate by testing for interactions between each climate variable and source elevation (as fixed effects), and genotype within population (as random slopes) in

generalized linear mixed models. We used the best-supported models to project λ_s under four climate scenarios: a preindustrial period (1850 to 1879), a contemporary period (2014 to 2022), and an end–21st century period (2071 to 2100) under an intermediate [Representative Concentration Pathway (RCP) 4.5] and a high-emissions pathway (RCP-8.5) based on down-scaled regional projections (*34*, *35*) (fig. S4).

Our models revealed strong local adaptation to climate (Fig. 1, F and G, and fig. S10). Most vital rates exhibited optimal climate conditions that varied significantly with source elevation, indicating that local adaptation to snowmelt and growing season temperature are major drivers of variation in fitness (tables S4 to S11 and figs. S6 to S8). By integrating across vital rates with genotype-specific IPMs, we estimated that each genotype achieved its peak fitness (highest λ) under distinct climates. The optimal snowmelt timing and growing season temperature mirrored the climate of origin (Fig. 1, F and G), reflecting elevational gradients in these climatic variables (figs. S4 and S10). Nevertheless, natural populations are not perfectly adapted to contemporary climates in their home sites. Rather, low-elevation genotypes show enhanced performance under later snowmelt and high-elevation genotypes could benefit from earlier snowmelt, and all genotypes are adapted to cooler temperatures than currently observed at their home sites (Fig. 1, F and G). Advancing snowmelt under climate change (fig. S4) could reduce fitness in low-elevation populations while increasing fitness in high-elevation populations, whereas increasing temperatures could depress fitness across the elevational range.

Local adaptation was most pronounced under preindustrial and contemporary climates, as λ_s (which incorporates realistic interannual climate variation) peaked when source elevations matched the elevation of each garden (Fig. 2A and table S12). Climate change is shifting the adaptive landscape to favor lower-elevation genotypes

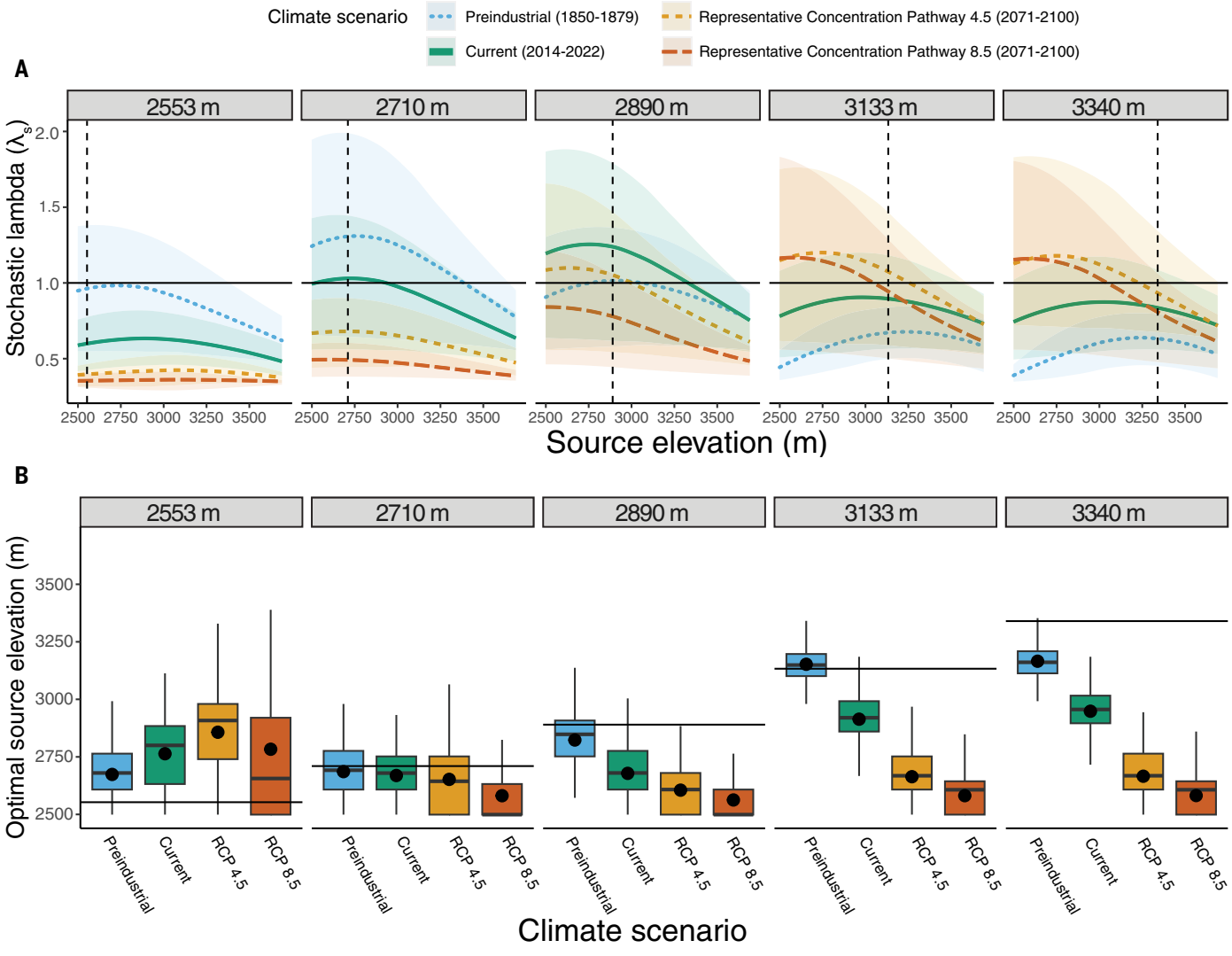

Fig. 2. Climate change disrupts local adaptation. (**A**) Stochastic lambda (λ_s; the geometric mean of λ across 1000 randomly sampled climate conditions for a given scenario), modeled from the Provenance Trial Experiment, varied with source elevation and climate scenario in five common gardens (elevations of the gardens in gray at the top of the panels; source elevations of genotypes on the *x* axis). Horizontal lines reflect $\lambda_s = 1$, at which populations are stable ($\lambda_s > 1$ indicates expanding populations and $\lambda_s < 1$ indicates contracting populations). Dashed vertical lines represent the garden elevation. Panels depict the fitness landscape under preindustrial climates (blue), contemporary climates (green), and end-of-century climates under intermediate emissions (orange) and worst-case emissions (red). Only low-elevation genotypes are predicted to reach $\lambda_s \geq 1$ in future climates in the three highest gardens, whereas all genotypes are predicted to have $\lambda_s << 1$ in future climates at the two lowest gardens. (**B**) The source elevation with the greatest λ_s under each climate scenario in each garden. Horizontal lines reflect the elevation of the garden. Box plots show the mean (circle), median (central line), first and third quartiles (box range), and the largest and smallest values within 1.5× the interquartile range (vertical lines) based on 1000 bootstraps. Under both future climate scenarios, the optimal source elevation is predicted to shift to much lower elevations across all gardens, indicative of local maladaptation.

while depressing the fitness of local genotypes (Fig. 2B and fig. S11). Our models predict significant extinction risks ($\lambda_s < 1$) at low- and even mid-elevation sites under both future climate scenarios (Fig. 2), suggesting substantial elevational range contractions. This prediction accords with our previous models in this system (*20*) and arises from the poor recent performance of transplants in our lowest-elevation garden (*37*). Furthermore, under both future climate scenarios, only low-elevation genotypes achieve $\lambda_s \geq 1$ in the mid-elevation and higher-elevation gardens, demonstrating that local populations are at risk of decline without the influx of migrants from lower elevations. That is, local extinctions may not be confined to marginal populations at the trailing edge of the range. Notably, contemporary high-elevation accessions are predicted to have poor performance ($\lambda_s < 1$) under preindustrial climates (Fig. 2A). Herbarium records in elevations >3200 m in the 1800s (*38*) indicate that high-elevation populations were present at that time. Thus we postulate that colder-adapted genotypes that performed best under preindustrial conditions may have already been lost from high-elevation locales owing to recent climate change.

Upslope gene flow is insufficient to keep pace with climate change

Populations in the historically cooler portion of the range could persist through climate change because of the immigration of genotypes preadapted to elevated temperatures from populations in historically warmer regions (*25*, *39*). Although *B. stricta*, like other species, recolonized high-elevation ecosystems after the retreat of the Pleistocene glaciers (*40*), climate change is likely outpacing recent rates of migration in plants and animals inhabiting mountainous ecosystems (*2*). We leveraged genotype-specific stochastic IPMs to examine how far genotypes would need to migrate to maintain stable local populations under four climate scenarios (Fig. 3A). We compared λ_s of all genotypes in the home site of each source population and calculated the closest genotype that could persist ($\lambda_s \geq 1$) in each climate scenario ("Climate Transfer Analysis").

Little migration is necessary to persist at lower elevations in preindustrial or contemporary climates, as local genotypes generally exhibit stable growth rates ($\lambda_s \geq 1$). However, upslope migration is necessary to maintain high-elevation populations under contemporary climates. Under the two end-of-century climate scenarios, most populations across the species' elevational range are predicted to require migrants from lower elevations to persist (Fig. 3A and tables S12 and S13). Upslope migration could rescue higher-elevation populations while conserving the low-elevation genotypes that are specifically adapted to projected climates.

To evaluate whether rates of upslope gene flow in *B. stricta* would be sufficient to enable population persistence across this elevational gradient, we established three elevational transects across separate mountains and inferred the best-fit long-term demographic models using genomic data (figs. S12 to S15 and table S13). We extracted DNA from 95 accessions across these transects and used an Illumina NextSeq 500 platform to generate low-coverage sequence data (average coverage 2.1×), and fit models using GADMA2 with the "moments" engine (*41*).

Gene flow in this system is spatially restricted, and contemporary levels of gene flow are unlikely to rescue high-elevation populations in the face of climate change. Minimum dispersal distances estimated from IPMs (Fig. 3A) predict that 96.9 m (±73.1, standard deviation) or 138.7 m (±67.8, standard deviation) of upslope migration would be necessary between now and 2071–2100 to maintain stable high-elevation populations in these three transects in the intermediate and worst-case emissions scenarios, respectively (table S13). However, models based on genomic sequence data show no upslope migration in the most recent epoch (Fig. 3B and figs. S12 to S15). This result suggests that natural gene flow alone will not be sufficient to keep pace with rapidly changing climates in this region.

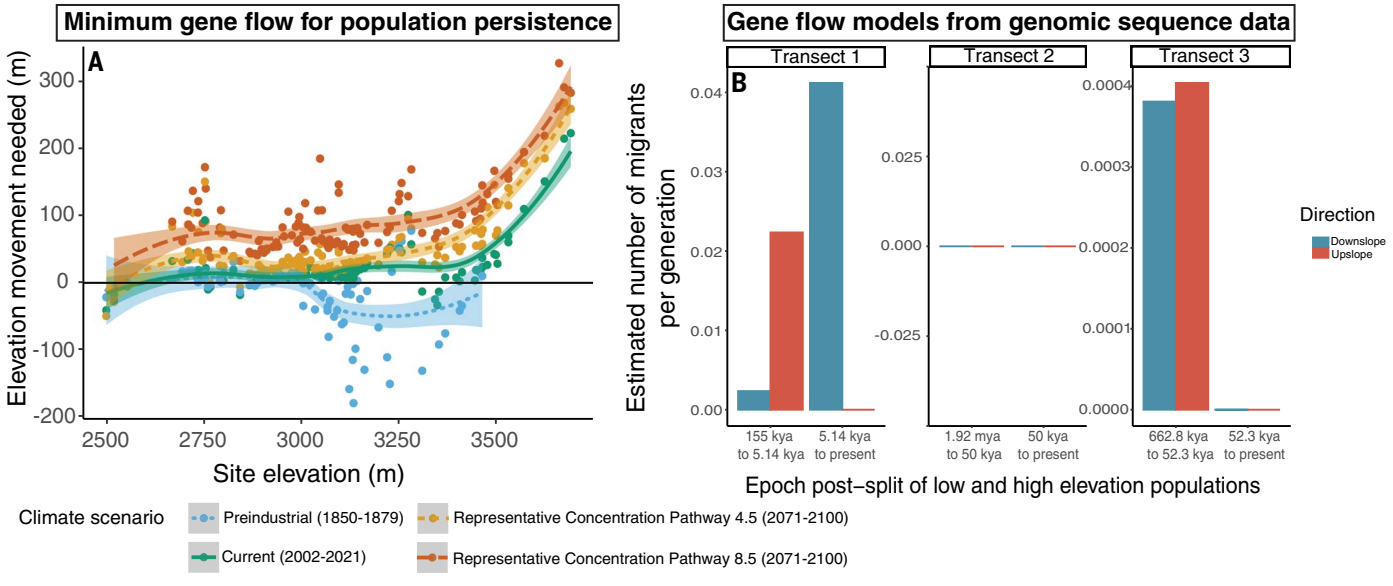

Fig. 3. Gene flow is unlikely to rescue local populations. (**A**) From integral projection models using data from the Provenance Trial Experiment, we calculated the movement necessary to maintain long-term persistence ($\lambda_s \geq 1$) for populations distributed across the elevational gradient under four climate scenarios. Positive values reflect the number of meters of upslope migration required, whereas negative values indicate that downslope migration would be necessary. In preindustrial climates, the highest elevation sites are predicted to have either been inhospitable to any currently available genotype (>3500 m) or to require migrants from even higher elevations to persist (~3000 to 3500 m), indicating a potential loss of the coldest-adapted genotypes from contemporary high-elevation accessions. In contemporary and future climates, IPMs indicate that genotypes from lower-elevation source populations could rescue higher-elevation populations, but our (**B**) genomic models indicate that gene flow is spatially restricted, with no upslope gene flow detected in the most recent epoch in any of the transects. Confidence intervals are so small that they cannot be seen. The population genomic demographic models with the moments engine of GADMA2 (*41*), which uses allele frequency spectrum (AFS) data, supported single ancestral populations that split into low- and high-elevation populations in all three transects (figs. S12 to S15). After this division, the models identified two epochs in each transect with different demographic histories and population sizes. The contemporary time frame is the most relevant to predicting gene flow patterns across current populations.

These results are not surprising, as *B. stricta* is primarily self-pollinating (*42*) and has dehiscent fruits that release gravity-dispersed seeds. In the absence of gene flow, our models predict that climate change could cause the elevational range to contract and could eliminate the low-elevation ecotypes that are best adapted to withstand new climates.

Reciprocal transplant experiment demonstrates limited potential for evolutionary rescue

Rapid adaptation could also allow populations to persist in forecasted climates (*23*, *24*). The rate of in situ adaptation depends on the extent of genetic variance in fitness within populations (*43*). To predict the adaptive potential of populations to climate change, we must consider genetic variance in fitness under projected climates. Some populations likely lack sufficient genetic variation to adapt to climate change (*12*, *44*), whereas others harbor cryptic genetic variation that emerges when exposed to new conditions (*23*, *45*). Environmental change could expose this cryptic genetic variation to selection, potentially hastening adaptive evolution (*23*, *24*). Nevertheless, we still know little about the extent of cryptic genetic variation or its importance in natural populations facing new environments (*45*).

Our provenance trial experiment revealed that range-wide genotypic variance in λ is highest under intermediate to delayed snowmelt timing and low growing-season temperature, with steep declines under projected future climates (Fig. 4A and fig. S16). Correspondingly, range-wide genotypic variance in λ_s is predicted to decline sharply in future climates in low- and mid-elevation sites (Fig. 4C and fig. S17). To evaluate the degree of within-population genotypic variation, we conducted a reciprocal transplant experiment, exposing a larger number of local genotypes to contemporary conditions and early snow removal in all gardens ($N = 11{,}850$ seeds from 124 genotypes, 17 to 30 genotypes per population, transplanted in fall 2015 and censused through fall 2018; $N = 6898$ juvenile rosettes from 122 accessions, 15 to 30 genotypes per population, transplanted in fall 2016 and censused through fall 2022; tables S14 to S15). We tested for interactions between each climate variable and source population (as fixed effects), and genotype within population (as random slopes) in generalized linear mixed models for each vital rate (tables S16) and constructed population- and genotype-specific IPMs to project λ as a function of climate and λ_s in preindustrial, contemporary, and future stochastic climate scenarios.

We found strong support for population and genotypic variation in climate responses in most vital rates in the Reciprocal Transplant

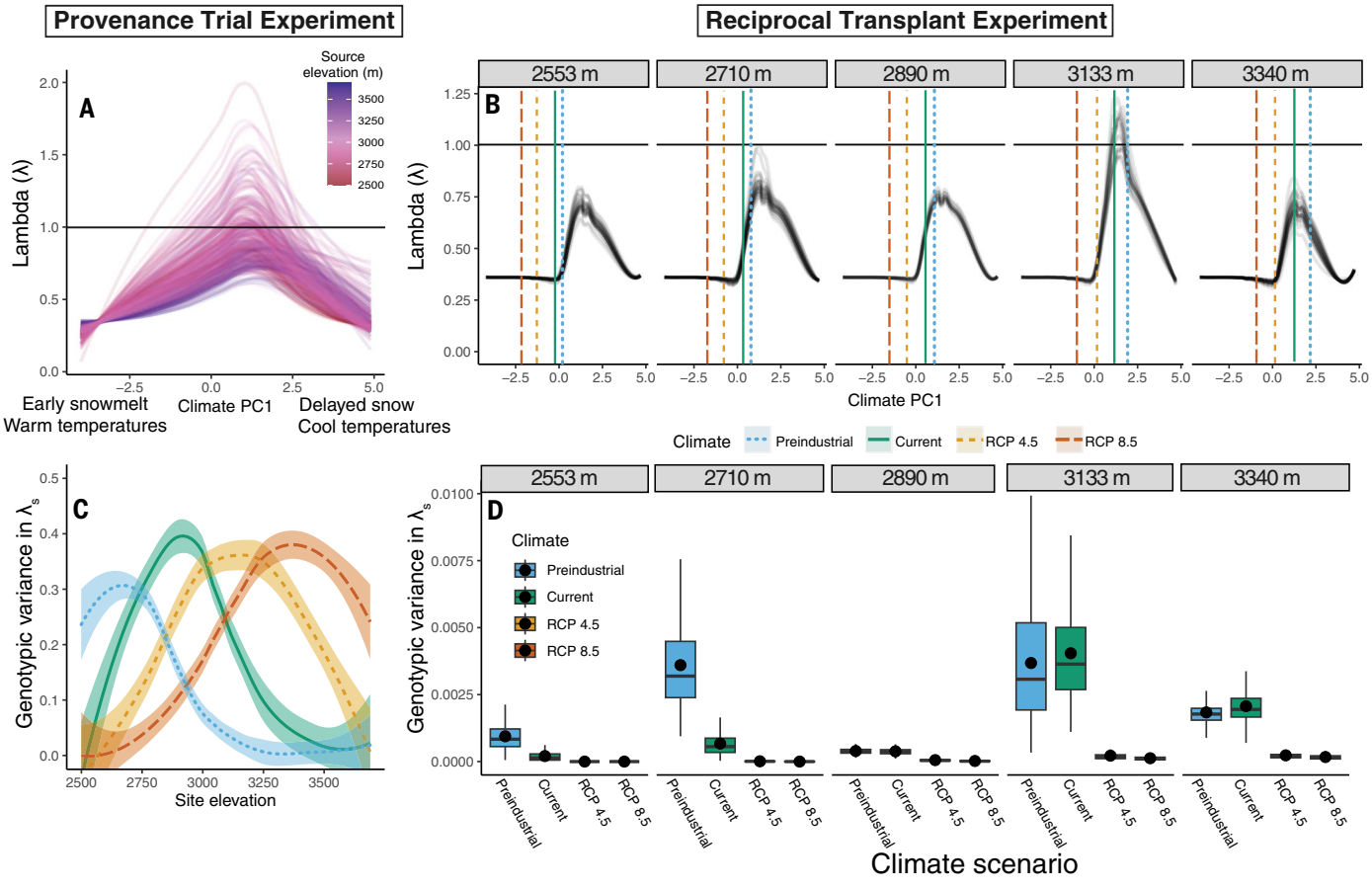

Fig. 4. Climate change reduces adaptive potential. Climatic performance curves for (**A**) all genotypes from the Provenance Trial Experiment and (**B**) local genotypes in each garden from the Reciprocal Transplant Experiment in response to climatic variation. Here, we combine snowmelt timing and growing season temperature in a principal component analysis; figs. S16 (Provenance Trial) and S21 (Reciprocal Transplant Experiment) show separate curves for each climatic variable. Low values of principal component 1 (Climate PC1) represent warm temperatures and early snowmelt and high values reflect cool temperatures and delayed snowmelt. The horizontal line signifies $\lambda = 1$, and vertical lines in (B) indicate local climates under four scenarios. (**C**) Genotypic variance in stochastic lambda (λ_s) across all genotypes of the provenance experiment if they were transplanted into each source location, capturing range-wide adaptive potential, which varies with climate scenario and site elevation. (**D**) Genotypic variance in λ_s for local genotypes from the reciprocal transplant experiment at each garden modeled under four climate scenarios. Box plots depict the mean (circle), median (central line), first and third quartiles (box range), and the largest and smallest values within 1.5× the interquartile range (vertical lines). Limited genotypic variance in λ_s, especially under projected future climates, could restrict adaptation of local populations from standing genetic variation.

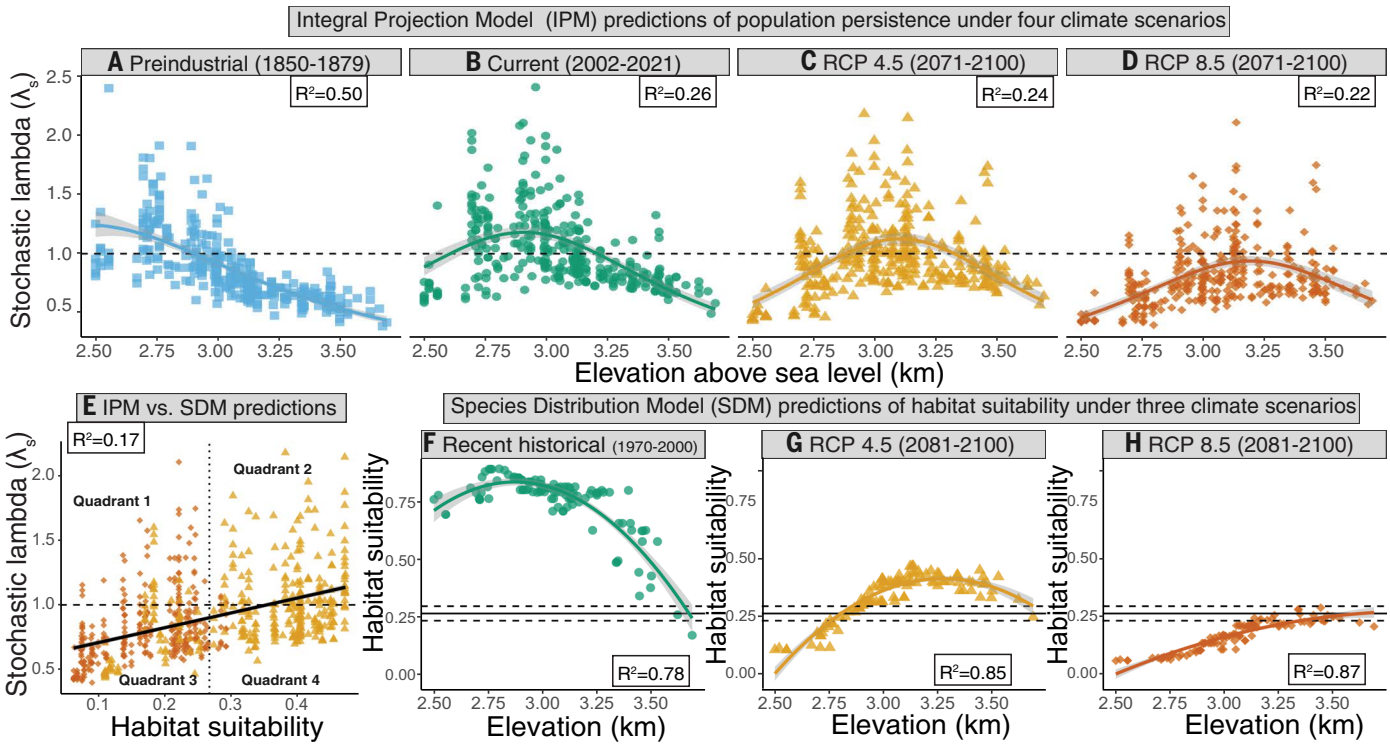

Fig. 5. Integral projection model (IPM) versus ensemble species distribution model (SDM) predictions of population persistence. Predictions of stochastic lambda (λ_s) using data from the Provenance Trial for each source population in its home site under (**A**) preindustrial climates, showing greatest performance of low-elevation populations; (**B**) current climates, revealing contractions at the lower elevational range and expansion at higher elevations, consistent with biogeographic shifts for a diversity of species (*2*); and (**C**) intermediate emissions scenarios, predicting upward shifts in the distribution and (**D**) worst-case emissions scenarios, predicting broad-scale population contractions. (**E**) Contrasts of IPM and SDM predictions under future climate scenarios. The horizontal dashed line shows $\lambda_s = 1$, and the vertical dotted line reflects the habitat suitability threshold for *B. stricta* persistence across 60 models in the ensemble SDM. In quadrants 2 and 3, the two approaches generate similar outcomes. In quadrant 1, IPMs predict persistence whereas SDMs predict extinction. The populations present in quadrant 4 are predicted to persist by SDMs but contract by IPMs. (**F**) SDMs for recent historical climates show high habitat suitability across the elevational range. Discrepancies between (B) and (F) could arise because BioClim data are not available range-wide for current climates (*50*). The habitat suitability threshold and 95% CI are indicated with solid and dashed lines, respectively. SDMs predict (**G**) population loss only at low elevations in the intermediate emissions scenario, and (**H**) large-scale extirpations in the high-emissions scenario.

Experiment (tables S16 to S24 and figs. S18 to S20). Integrating across vital rates in the Reciprocal Transplant Experiment revealed that genotypic variation in λ_s was greatest under preindustrial to contemporary climate conditions (Fig. 4, B and D; fig. S21; and table S25). As the climate shifts toward earlier snowmelt and warmer temperatures, within-population genotypic variation in λ_s diminished to negligible levels for all source populations (Fig. 4D).

By projecting λ_s of populations, allowing for evolution of genotype frequencies, we showed that local adaptive potential is insufficient for evolutionary rescue under future climates (fig. S22 and table S26). These evolutionary IPMs (*46*) evaluate the potential for evolutionary rescue by incorporating genotype as a state variable to allow for realistic changes in genotype frequencies over time driven by differences in their relative fitness. Concordant with thermal performance curves (*47*), genotype-specific climatic niches were often asymmetrical, suggesting that small increases in growing season temperature and accelerations in snowmelt timing will result in steep declines in λ (Fig. 4C and fig. S22). This limited genetic variation under early snowmelt and elevated temperatures suggests that cryptic genetic variation will likely not enable rapid evolution of local *B. stricta* populations to new climates.

Species distribution models could generate unreliable forecasts

Species distribution models (SDMs) are widely used for forecasting distributions under climate change. To evaluate the degree to which SDMs reflect complex population dynamics, we modeled habitat suitability on the basis of bioclimatic parameters from the localities of 156 known *B. stricta* populations in Colorado plus 496 background points, using 30–arc sec resolution environmental variables from WorldClim2.1 (*48*) for near historical (1970–2000) and future climate scenarios (2081–2100; Fig. 1, fig. S2, and table S27).

Ensemble SDMs predict high habitat suitability for Colorado populations that demographic models suggest will contract under the RCP 4.5 climate scenario (Fig. 5E). However, consistent with IPMs (Fig. 5, A to D), the ensemble SDM forecasts population contractions in the lower elevational range (Fig. 5, G and H). Differences in the core assumptions of these approaches could underlie divergent forecasts. Species distribution models estimate the climatic niche for the entire species and predict whether a location is suitable for any accession (*49*). Thus, SDMs assume limited local adaptation and unrestricted migration, whereas IPMs can be constructed to account for local adaptation. Furthermore, SDMs built using near-historical climatic and occurrence data (e.g., from herbarium or museum specimen) may poorly reflect contemporary population dynamics under climate change (*50*), whereas IPMs capture fitness responses to fine-grained environmental variation that is not represented even in the highest-resolution bioclimatic parameters from WorldClim (*48*). Finally, the regressions of habitat suitability from SDMs versus site elevation have substantially higher R-squared values compared with models of stochastic lambdas versus site elevation for the same populations, which could lead researchers to overestimate the predictive power of these models.

Conclusions

Determining the contributions of climatic factors to local adaptation is crucial for forecasting population persistence under future climates, predicting loss of intraspecific genetic diversity, determining whether preadapted ecotypes exist in trailing-edge populations, and drafting informed conservation practices. Here, we show that climate change increases the risk of extinction of locally adapted populations while decreasing adaptive potential and outpacing gene flow, even in a common and widely distributed species.

Gene flow is likely much higher in outcrossing species and those with mixed mating systems, yet even in those systems, it is critical to examine the directionality of gene flow. For example, in the mountains of Norway, asymmetrical downslope gene flow prevails in the self-incompatible *Arabidopsis lyrata* (*51*). Furthermore, syntheses suggest that climate change is outpacing recent rates of upslope migration in plants and animals inhabiting mountainous ecosystems, likely owing to limited dispersal capacity, biotic interactions, and microtopographic variation that generates local thermal refugia (*2*). Assisted gene flow (*52*) may be an efficient strategy for conserving genetic diversity and enhancing persistence of montane species, as long as protocols account for local adaptation to nonclimatic conditions (*53*).

Forecasting approaches that do not account for intraspecific climatic specialization, genetic variation under new climates, and gene flow could miss key avenues for conservation, neglect the importance of assisted gene flow for leading-edge populations, and fail to consider the specific adaptations of trailing-edge ecotypes to future climates. Species distribution models may perform well for highly mobile species with low levels of local adaptation but could generate biased predictions and lead to poor conservation practices for species with locally adapted populations. For example, the demographic models alone suggest that assisted migration could reduce the risk of extinction in future climates. Finally, our models generated markedly different predictions under the two future climate scenarios, highlighting that reductions in greenhouse gas emissions remain a powerful strategy for preserving genetic diversity.

REFERENCES AND NOTES

1. J. Lenoir *et al.*, *Nat. Ecol. Evol.* **4**, 1044–1059 (2020).
2. W.-P. Chan *et al.*, *Nature* **629**, 114–120 (2024).
3. J. Ehrlén, W. F. Morris, *Ecol. Lett.* **18**, 303–314 (2015).
4. J. Gurevitch, G. A. Fox, N. L. Fowler, C. H. Graham, *Q. Rev. Biol.* **91**, 459–485 (2016).
5. C. Merow *et al.*, *Ecography* **37**, 1167–1183 (2014).
6. T. E. X. Miller *et al.*, *Ecology* **101**, e03139 (2020).
7. W. Thuiller *et al.*, *Ecol. Lett.* **16** (Suppl 1), 94–105 (2013).
8. J. R. Lasky, M. B. Hooten, P. B. Adler, *Proc. Biol. Sci.* **287**, 20202219 (2020).
9. A. S. A. Johnston *et al.*, *Proc. Biol. Sci.* **286**, 20191916 (2019).
10. S. N. Sheth, A. L. Angert, *Evolution* **68**, 2917–2931 (2014).
11. K. S. Sheldon, R. B. Huey, M. Kaspari, N. J. Sanders, *Am. Nat.* **191**, 553–565 (2018).
12. V. Kellermann, B. van Heerwaarden, C. M. Sgrò, A. A. Hoffmann, *Science* **325**, 1244–1246 (2009).
13. R. Leimu, M. Fischer, *PLOS ONE* **3**, e4010 (2008).
14. J. Hereford, *Am. Nat.* **173**, 579–588 (2009).
15. D. R. Campbell, J. M. Powers, *Proc. Biol. Sci.* **282**, 20150178 (2015).
16. E. Hamann, A. E. Weis, S. J. Franks, *Evolution* **72**, 2682–2696 (2018).
17. T. Wang, G. A. O'Neill, S. N. Aitken, *Ecol. Appl.* **20**, 153–163 (2010).
18. A. M. Wilczek, M. D. Cooper, T. M. Korves, J. Schmitt, *Proc. Natl. Acad. Sci. U.S.A.* **111**, 7906–7913 (2014).
19. N. J. Kooyers *et al.*, *Am. Nat.* **194**, 541–557 (2019).
20. J. T. Anderson, S. M. Wadgymar, *Ecol. Lett.* **23**, 181–192 (2020).
21. A. J. Gorton, J. W. Benning, P. Tiffin, D. A. Moeller, *Evolution* **76**, 2916–2929 (2022).
22. S. M. Carlson, C. J. Cunningham, P. A. Westley, *Trends Ecol. Evol.* **29**, 521–530 (2014).
23. M. C. Bitter, L. Kapsenberg, J.-P. Gattuso, C. A. Pfister, *Nat. Commun.* **10**, 5821 (2019).
24. J. Zheng, J. L. Payne, A. Wagner, *Science* **365**, 347–353 (2019).
25. M. Bontrager, A. L. Angert, *Evol. Lett.* **3**, 55–68 (2018).
26. I. A. Al-Shehbaz, M. D. Windham, "Boechera" in *Flora of North America North of Mexico*, Flora of North America Editorial Committee, Ed. (Oxford Univ. Press, 2010), pp. 348–412.
27. H. A. Nomoto, J. M. Alexander, *Ecol. Lett.* **24**, 1157–1166 (2021).
28. Mountain Research Initiative, *Nat. Clim. Chang.* **5**, 424–430 (2015).
29. Methods and materials are available as supplementary materials.
30. S. P. P. Ellner, D. Z. Childs, M. Rees, *Data-Driven Modelling of Structured Populations: A Practical Guide to the Integral Projection Model Lecture Notes on Mathematical Modelling in the Life Sciences* (Springer, 2016).
31. R. Wooliver, E. E. Vtipilthorpe, A. M. Wiegmann, S. N. Sheth, *AoB Plants* **14**, plac016 (2022).
32. S. C. Stearns, *Evolution of Life Histories* (Oxford Univ. Press, 1992).
33. D. R. Campbell, *Proc. Natl. Acad. Sci. U.S.A.* **116**, 12901–12906 (2019).
34. V. Masson-Delmotte et al., Eds., *Climate Change 2021: The Physical Science Basis. Contribution of Working Group I to the Sixth Assessment Report of the Intergovernmental Panel on Climate Change* (Cambridge Univ. Press, 2023).
35. A. C. Lute, J. Abatzoglou, T. Link, *Geosci. Model Dev.* **15**, 5045–5071 (2022).
36. C. J. Talsma, K. E. Bennett, V. V. Vesselinov, *Earth Space Sci.* **9**, e2021EA002086 (2022).
37. J. Anderson, M. DeMarche, Boechera stricta climate change dataset, Zenodo (2024); https://doi.org/10.5281/zenodo.14659942.
38. Biodiversity occurrence data published by the Consortium of Intermountain Herbaria (2025); https://intermountainbiota.org/portal (accessed 12 January 2025).
39. A. Hampe, R. J. Petit, *Ecol. Lett.* **8**, 461–467 (2005).
40. C. Kiefer, C. Dobeš, T. F. Sharbel, M. A. Koch, *Mol. Phylogenet. Evol.* **52**, 303–311 (2009).
41. E. Noskova *et al.*, *Gigascience* **12**, giad059 (2022).
42. B.-H. Song, M. J. Clauss, A. Pepper, T. Mitchell-Olds, *Mol. Ecol.* **15**, 357–369 (2006).
43. R. A. Fisher, *The Genetical Theory of Natural Selection* (Oxford Univ. Press, 1930).
44. M. Exposito-Alonso *et al.*, *Science* **377**, 1431–1435 (2022).
45. A. B. Paaby, M. V. Rockman, *Nat. Rev. Genet.* **15**, 247–258 (2014).
46. M. Rees, S. P. Ellner, *Methods Ecol. Evol.* **7**, 157–170 (2016).
47. T. L. Martin, R. B. Huey, *Am. Nat.* **171**, E102–E118 (2008).
48. S. E. Fick, R. J. Hijmans, *Int. J. Climatol.* **37**, 4302–4315 (2017).
49. D. Zurell *et al.*, *Ecography* **43**, 1261–1277 (2020).
50. J. Lee-Yaw, J. McCune, S. Pironon, S. N. Sheth, *Ecography* **2022**, e05877 (2022).
51. T. Hämälä, O. Savolainen, *Mol. Biol. Evol.* **36**, 2557–2571 (2019).
52. S. N. Aitken, M. C. Whitlock, *Annu. Rev. Ecol. Evol. Syst.* **44**, 367–388 (2013).
53. A. Bucharova, *Restor. Ecol.* **25**, 14–18 (2017).

ACKNOWLEDGMENTS

We are grateful for J. Reithel's assistance with logistics for the field experiments. The Rocky Mountain Biological Laboratory, the Crested Butte Land Trust and Estess family allowed us to conduct common garden experiments on their land. We thank the expert backcountry skiers who conducted the snow removals, field researchers for their assistance collecting vital rate data, and greenhouse staff who assisted with growing plants prior to transplanting, including M. Robbins, I. Jameel, S. Day, B. Chowdhury, C. Daws, A. Battiata, C. Boerner, T. Morrison, S. Srivatsan, N. Workman, H. Nagle, M. Boyd, K. Tarner, D. Proudfoot, T. Kilgore, C. Smith, A. Beason, B. Ammon, A. Tiberio, P. Innes, K. Haner, A. Esparza, D. Eldridge, H. Grimess, E. Cheslock, E. Ross, R. MacTavish, A. Bohon, J. Adachi, J. Gall, M. Verner-Crist, M. Manto, and C. Beutler. V Ezenwa, M. Geber, D. Doak, S. Sheth, and B. Schmitz commented on a previous draft, and T. Pendergast assisted with model runs on the cluster, helped with data collection and garden maintenance, and provided feedback on the manuscript. We are grateful for the comments of two anonymous reviewers on a previous draft. B. Chowdhury and J. Gall granted permission to use photographs 1, 2, and 5 in Fig. 1E. **Funding:** Fieldwork and data collection for this study were funded by the National Science Foundation (DEB-1553408 to J.T.A.). A separate award from the National Science Foundation (IOS-2220927 to J.T.A. and M.L.D.) aided in the conceptualization of this study. **Author contributions:** Conceptualization: J.T.A., M.L.D. Methodology: J.T.A., M.L.D., I.B., D.A.D., J.S., S.M.W. Investigation: J.T.A., M.L.D., I.B., D.A.D., J.S., S.M.W. Visualization: J.T.A., M.L.D., D.A.D., J.S. Funding acquisition: J.T.A. Project administration: J.T.A. Supervision: J.T.A. Writing – original draft: J.T.A., M.L.D., I.B., D.A.D., J.S. Writing – review & editing: J.T.A., M.L.D., I.B., D.A.D., J.S., S.M.W. **Competing interests:** The authors declare that they have no competing interests. **Data and materials availability:** Data, code, and output files from the integral projection models are available in Zenodo from reference (*37*). That repository includes data for the provenance trial and reciprocal transplant experiments and code for the vital rate models, integral projection models, associated figures, species distribution models, and code for gene flow models. Genomic data for the gene flow analyses are available at GenBank (BioProject: PRJNA1123727).

SUPPLEMENTARY MATERIALS

science.org/doi/10.1126/science.adr1010
Materials and Methods; Supplementary Text; Figs. S1 to S25; Tables S1 to S27; References (*54*–*146*); MDAR Reproducibility Checklist

Submitted 14 June 2024; accepted 7 March 2025

10.1126/science.adr1010